Available online at www.sciencedirect.com
ScienceDirect
Journal of the European Ceramic Society 30 (2010) 2491–2496
www.elsevier.com/locate/jeurceramsoc

Thermal expansion of EB-PVD yttria stabilized zirconia

R. Ochrombel [a,*], J. Schneider [b], B. Hildmann [a], B. Saruhan [a]

[a] DLR, German Aerospace Center, Institute of Materials Research, D-51170 Cologne, Germany
[b] Section Crystallographie, Ludwig-Maximilians-University Munich, D-80333 Munich, Germany

Received 3 August 2009; received in revised form 3 May 2010; accepted 16 May 2010

Abstract

Yttria stabilized zirconia (YSZ) layers, suited for thermal barrier coatings (TBCs) in turbine engines, were produced by electron-beam physical vapour deposition (EB-PVD) on metallic (Ni-based alloys) ceramic (Al_2O_3) substrates (typically at 1000 °C) using ingot compositions of about 4 mol% Y_2O_3–ZrO_2. Employing powdered samples, removed from the surface of the as-deposited YSZ layers, precision X-ray diffraction data sets were recorded between 60 and 900 °C and the lattice parameters of the metastable, tetragonal (t′) and the cubic (c) phases were refined using Rietveld's method. It was unambiguously verified that phase (c) was present in all investigated samples as a minority phase already in the as-deposited state.

The thermal expansion coefficients of the tetragonal phase (t′) ($\alpha_{11} = 9.3(2) \times 10^{-6}\,K^{-1}$, $\alpha_{33} = 10.8(1) \times 10^{-6}\,K^{-1}$) and the cubic phase (c) ($\alpha_{11} = 8.5(2) \times 10^{-6}\,K^{-1}$) were evaluated from the refined temperature dependent lattice parameter values of this study, and turned out to be close to each other, but significantly different from the coefficient of the monoclinic phase (m) ($\alpha_{11} = 9.0 \times 10^{-6}\,K^{-1}$, $\alpha_{22} = 1.2 \times 10^{-6}\,K^{-1}$, $\alpha_{33} = 11.9 \times 10^{-6}\,K^{-1}$, $\alpha_{13} = 0.0 \times 10^{-6}\,K^{-1}$), which was derived from temperature dependent lattice parameter measurements published by Touloukian et al.[5] The expansion coefficient of the monoclinic phase (m) exhibited a very pronounced anisotropy in contrast to the tetragonal phases (t′) and (t). Our values for (t′) and (c) were in excellent agreement with that of other tetragonal and cubic phases from the literature with quite different Y_2O_3 contents.

Keywords: Y_2O_3; ZrO_2; X-ray methods; Thermal expansion

1. Introduction

Thermal barrier coatings (TBCs) deposited on metallic turbine blades are used as a viable additional method to the air cooling system to increase the inlet temperature in turbines of aero-engines in order to improve the efficiency of the turbines. The electron-beam physical vapour deposition (EB-PVD) method is meanwhile an established manufacturing process to produce light-weight coatings with an efficient combination of thermo-mechanical properties required for aero-engine turbines. Today the state of the art material for EB-PVD TBCs is yttria stabilized zirconia (YSZ). Different polymorphs of YSZ can be obtained by varying the yttria content. As shown in the ZrO_2–Y_2O_3 equilibrium phase diagram by Scott,[1] at a composition of 4 mol% Y_2O_3–ZrO_2 two different stable two-phase regions occur as a function of temperature: either a mixture of monoclinic (m) and cubic (c) phases at temperatures below 565 °C, or a mixture of cubic (c) and tetragonal (t) phases at temperatures above 565 °C.

However, employing a 4 mol% Y_2O_3–ZrO_2 target in an EB-PVD process the rapid condensation of the vapour species and crystallization on top of a relatively cold substrate (typically 1000 °C) generally generate a non-equilibrium tetragonal mixed crystal phase (t′) as majority phase with the Y_2O_3 concentration close to, but somewhat smaller than, that of the target and clearly higher than that of the equilibrium tetragonal mixed crystal phase (t). In addition to phase (t′), a cubic phase (c) is produced during the EB-PVD process as minority phase with a higher Y_2O_3 concentration than that of the target. The presence of phase (c) is discussed somewhat contrarily in the literature. The YSZ phase (t′) stays stable, or better said stabilized between room temperature and ≈1100 °C and is also designated as partially stabilized zirconia (PSZ), because at temperatures above ≈1200 °C it decomposes according to the reaction (t′) → (t) + (c) in a ther-

* Corresponding author.
E-mail address: rene.ochrombel@web.de (R. Ochrombel).

0955-2219/$ – see front matter © 2010 Elsevier Ltd. All rights reserved.
doi:10.1016/j.jeurceramsoc.2010.05.008

mally activated process. The cubic YSZ phase (c) is designated as fully stabilized zirconia (FSZ) above a content of ≈9 mol% Y_2O_3, because it stays stable from room temperature to the melting point. The tetragonal YSZ phase (t′) and (t) crystallises in space group $P4_2/nmc$. The cubic YSZ phase (c) crystallises in space group $Fm3m$.

Thermal expansion depends both on the yttria content and the resulting phase. The knowledge of thermal expansion of YSZ materials plays a key-role for understanding deformation, microstructure and crack formation in EB-PVD TBCs. It is remarkable, that in the literature only little is known about the thermal expansion coefficients of technically used YSZ with an overall yttria content of ≈4 mol% Y_2O_3. Moreover published data for the thermal expansion of different zirconia polymorphs, especially of those stabilized with lower yttria contents, are partially inconsistent.

In this study we focus on the determination of the temperature dependent lattice parameters and thereby of the thermal expansion coefficients of the stabilized tetragonal phase (t′) and of the cubic phase (c) up to 900 °C by means of precision X-ray powder diffraction and data evaluation via Rietveld's method. This procedure leads to detailed information on qualitative and quantitative phase analyses and on thermal properties of the phases involved. Since in the present study the properties of the as-deposited metastable phase (t′) and phase (c) should be analysed, the in situ X-ray diffraction experiments stayed below the critical transformation temperature region.

2. Experimental procedure

2.1. YSZ sample preparation

In this study flat α-Al_2O_3 substrates (15 mm × 30 mm) were used to deposit about 400 μm thick YSZ layers by reactive EB-PVD under standard conditions employing an ingot rod with an average composition of 4 mol% Y_2O_3-ZrO_2 (TRANSTECH USA). The ceramic subtrate temperature was 1000 °C at a deposition rate of 3 μm/min on the rotating pin. The coating equipment used in the present study was a 150 kW EB-PVD coater (ARDENNE Anlagetechnik GmbH pilot plant) with separate chambers for loading, preheating, and deposition (for detailed description see Ref. 2). For comparison, further YSZ layers were deposited on a cooled steel substrate, attached to the process chamber wall, under otherwise unchanged experimental EB-PVD conditions.

2.2. X-ray diffraction and Rietveld refinement procedures

For X-ray diffraction (XRD) experiments polycrystalline samples were mechanically removed from the surface of the YSZ layers, deposited on top of α-Al_2O_3 and steel substrates. The samples were ground to fine powders in an agate mortar in order to avoid texture effects. The powders were filled in quartz capillaries of 0.5 mm diameter. XRD pattern between 60 and 900 °C (at 60 °C then at 100 °C followed by 100 °C intervals) were recorded using a precision X-ray powder diffractometer (STOE STADI P, Stoe, Darmstadt, Germany) equipped with a detector image plate employing monochromatic MoKα$_1$ radiation. The YSZ samples were heated by an in situ high temperature oven, furnished with graphite heating elements, and operated under Ar inert gas. The heating rate between measuring points was 2 °C/min. The data collection at each measuring temperature needed approximately 30 min. Diffraction pattern were obtained within $2\theta = 20$–56° range in 0.02° steps using standard θ–2θ Debye–Scherrer geometry. Lattice parameters and phase contents of the phases present in the samples were simultaneously refined applying Rietveld's method programmed in the computer routine WYRIET.[3] For experimental details see Table 1.

Table 1
Experimental XRD conditions.

Radiation type, source	X-ray, MoKα$_1$ (λ = 0.7093 Å)
Instrumental	STOE STADI P
Monocromator	Diffracted beam, Johann monocromator
Detector	Image plate
2θ range used in refinement	20–56°
Step size	0.02°
Phases	
t′-YSZ	SG: $P4_2$/nmc (No. 137)
c-YSZ	SG: Fm3m (No. 225)

The number after "*R*-factors" are: $R_p = 100\sum_i |y_i - y_{ci}| / \sum_i |y_i|$, the pattern *R*-factor, $R_{wp} = 100\sqrt{\sum_i w_i(y_i - y_{ci})^2 / \sum_i w_i y_i^2}$, the weighted pattern R-factor, $R_{expected} = 100\sqrt{\sum_i (N - P + C) / \sum_i w_i y_i^2}$, S is the "goodness of fit", the ratio $R_{wp}/R_{expected}$, where $w_i = 1/y_i$, y_i is the observed (gross) intensity at the ith step, y_{ci} is the calculated intensity at the ith step.

2.3. Determination of thermal expansion

In most cases, far from a phase transition, the linear approximation turned out to be an adequate approach. The correlation of the crystallographic axes $\{\vec{a}_i\}$ with the axes of the cartesian basis system $\{\vec{e}_i\}$ to describe the expansion tensor is given by $\vec{e}_3 || \vec{a}_3$, $\vec{e}_2 || \vec{a}_3 \times \vec{a}_1$, $\vec{e}_1 || \vec{e}_2 \times \vec{e}_3$ (see Ref. 4). For the orthogonal crystal systems, i.e. the tetragonal and cubic phases of YSZ, the relations simplify to $\vec{e}_1 || \vec{a}_1$, $\vec{e}_2 || \vec{a}_2$, $\vec{e}_3 || \vec{a}_3$. In the monoclinic phase (crystal class 2/m, second setting: $\vec{e}_2 || \vec{a}_2 || 2$) zirconia exhibits four independent tensor components, whereas in the tetragonal (4/mmm) and in the cubic phase (m3m) there are only two and one components, respectively.

For the determination of thermal expansion coefficients the equation:

$$L'_i(T) = L'_i(T_0)(1 + \alpha'_{ii}(T - T_0)) \quad (1)$$

was used, where $\{\vec{e}'_i\}$ is the sample system, defined by $\vec{e}'_i = u_{ij}\vec{e}_j$, L'_i is the length, α'_{ij} is the linear thermal expansion coefficient.

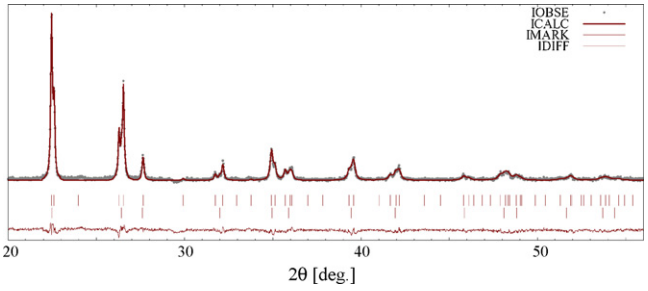

Fig. 1. Rietveld refinement of investigated X-ray powder pattern measured at $T = 600\,^{\circ}C$.

3. Results and discussion

The Rietveld refinements in this study verified that all analysed as-coated YSZ samples contained a two-phase mixture of a majority tetragonal (t′) and a minority cubic (c) phase. However, the superimposed X-ray diffraction pattern of the two phases overlapped almost completely over the entire 2θ region. At a first sight the samples seemed to contain only one single, tetragonal phase. Within the small 2θ interval 30.5–32.8° (MoKα_1) the reflections 004 (t′), 220 (t′) and 400 (c) were clearly separated in the XRD pattern (see Figs. 1 and 2). This fact implied that only via refinements of the entire XRD profiles (Rietveld's method) reliable data on the lattice parameters and the relative contents of the two phases could be obtained. Employing Voigt's profile type the XRD spectra were very well fitted for both samples and phases with R_p values all below 6%. The difference signals ($I_{diff} = I_{obs} - I_{calc}$) were relatively smooth even around the groups of overlapping diffraction lines (cf. pattern measured at 600 °C in Fig. 1). Note that the fitted profile section shown in Fig. 2 (solid line) belongs to the refinement over the entire XRD spectrum.

The results of the Rietveld refinements at various temperatures are summarized in Tables 2 and 3 and explain the overlapping of the XRD pattern. The temperature dependent development of the lattice parameters and phase contents measured at powders taken from the ceramic substrate are summarized in Table 3 and depicted in Fig. 3. The thermal expansion coefficients were calculated from data of Table 3. They are compared to literature data in Table 4.

In Fig. 4 the Full Width at Half Maximum values (FWHM) of tetragonal YSZ at two measuring temperatures are shown in dependence of the diffraction angle 2θ. It should be emphasized that the plotted FWHM values do not correspond to a superimposition of the two contributions originating from the tetragonal and the cubic phase of YSZ. The reason for that is due to the fact that in the Rietveld refinements both phases were treated separately resulting in two different sets of crystal structure data.

However, it was not possible to include the Y_2O_3 content of the individual phases (t′) and (c) as additional free parameter in the structure refinements because of very similar X-ray scattering factors of the Y and Zr atoms and strong correlation to the ADP parameters of the structure. Instead they were determined via Vegard's law published in the literature.

The analysis of the data to evaluate the effects of grain size and strain on peak broadening were performed using the

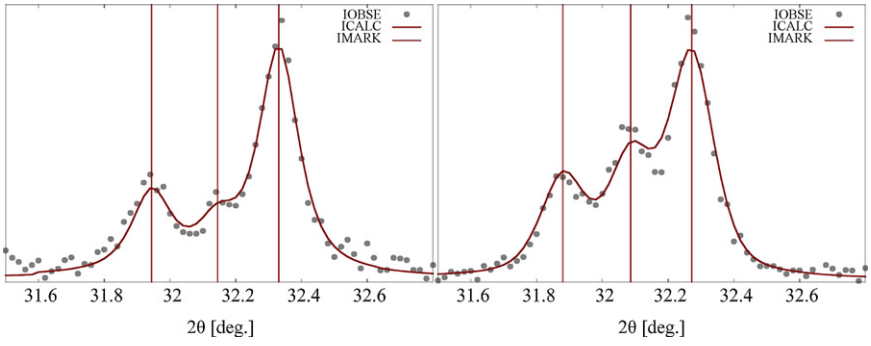

Fig. 2. Clearly resolved reflections 0 0 4 (t′), 2 2 0 (t′) and 4 0 0 (c) (at center) within the 2θ range 30.5–32.8° (MoKα_1). Left: sample from hot ceramic substrate (α-Al_2O_3) measured at $T = 60\,^{\circ}C$. Right: sample from cooled metallic substrate measured at $T = 20\,^{\circ}C$.

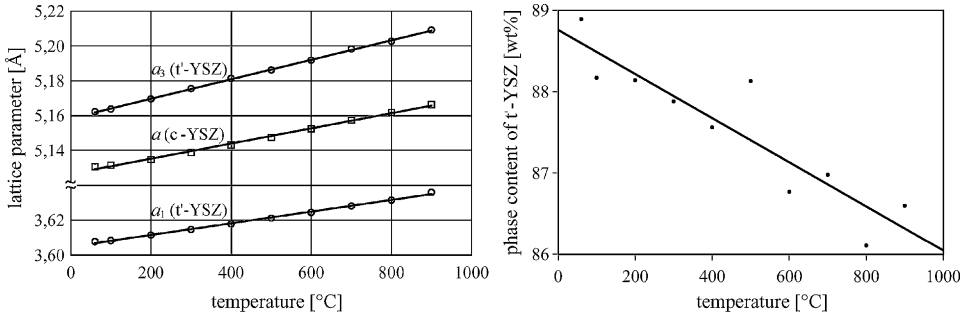

Fig. 3. Lattice parameters (left) and phase content (right) between 60 and 900 °C. a_1 (t′-YSZ) = 3.6048(3) + 3.35(6) × 10^{-5} T, a_3 (t′-YSZ) = 5.1585(3) + 5.58(5) × 10^{-5} T. a (c-YSZ) = 5.1266(5) + 4.35(10) × 10^{-5} T with T in [°C].

Table 2
Lattice parameters and phase content of powder taken from the cooled metallic substrate.

Temp. [°C]	a (c) [Å]	a_1 (t′) [Å]	a_3 (t′) [Å]	t′-YSZ [wt%]	c-YSZ [wt%]	R_p [%]	R_{wp} [%]	S
20	5.1341(2)	3.6100(1)	5.1644(3)	64.7(12)	35.3(11)	3.10	4.34	1.69

Table 3
Lattice parameters and phase content of powder taken from the ceramic subtrate at $T = 1000\,^{\circ}C$.

Temp. [°C]	a (c) [Å]	a_1 (t′) [Å]	a_3 (t′) [Å]	t′-YSZ [wt%]	c-YSZ [wt%]	R_p [%]	R_{wp} [%]	S
60	5.1307(9)	3.6077(4)	5.1622(6)	88.9(15)	11.1(9)	6.10	7.69	1.78
100	5.1315(9)	3.6082(4)	5.1638(6)	88.2(15)	11.8(9)	6.03	7.67	1.77
200	5.1347(9)	3.6114(4)	5.1695(6)	88.1(16)	11.9(2)	5.60	7.22	1.60
300	5.1388(9)	3.6146(4)	5.1755(6)	87.9(15)	12.1(9)	5.67	7.20	1.54
400	5.1431(9)	3.6178(4)	5.1813(7)	87.6(16)	12.4(9)	6.04	7.58	1.61
500	5.1475(9)	3.6211(4)	5.1861(6)	88.1(15)	11.9(9)	5.53	6.59	1.48
600	5.1525(10)	3.6244(5)	5.1918(7)	86.8(16)	13.2(9)	6.09	7.52	1.61
700	5.1574(10)	3.6281(5)	5.1982(8)	87.0(16)	13.0(9)	5.83	7.31	1.56
800	5.1619(10)	3.6315(5)	5.2026(8)	86.1(17)	13.9(10)	5.98	7.43	1.57
900	5.1663(11)	3.6360(6)	5.2091(9)	86.6(18)	13.4(11)	6.06	7.45	1.58

Numbers in parantethes correspond to estimated standard deviations and refer to the last digits.

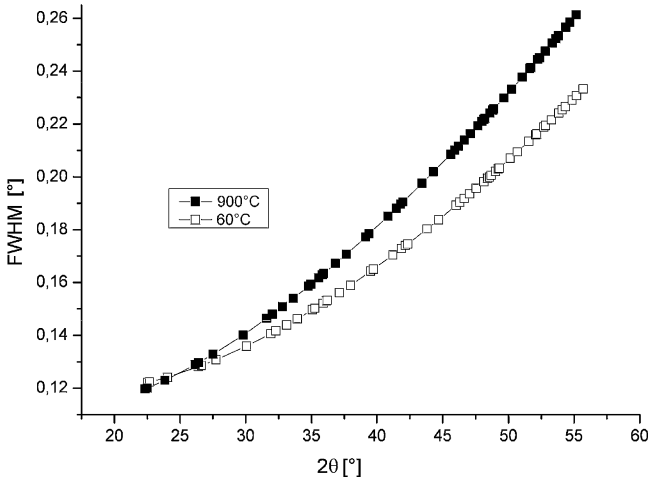

Fig. 4. Full width at half maximum values (FWHM) of tetragonal (t′)-YSZ at 60 °C and 900 °C plotted as a function of the diffraction angle 2θ. *Note*: Zero-point is suppressed.

Thomson–Cox–Hastings profile in addition to Voigt's profile (see Fig. 5). A narrow distribution of grain size between 650 and 780 Å, and a relatively small and almost constant value for strain as function of temperature were found. Both parameters grain size and strain remained unchanged during heating up to 900 °C.

The results of our study on thermal expansion coefficients of the two phases (t′) and (c) show that internal stresses and strains associated with temperature rise should be minimal, because both phases exhibit very similar thermal expansion coefficients.

Generally our refined lattice parameters of the tetragonal and cubic phases at room temperature are in good agreement with those from the literature, if the slightly different Yttria contents are taken into account. For the cubic phase we obtained a somewhat smaller value (about 0.01 Å) at room temperature than Ilavsky and Stalick[9] and Witz et al.[10] due to clearly lower yttria content in our samples. In all recent publications, including the present one, the yttria content was determined using an established Vegard's law for the cubic phase:

$$YO_{1.5}\,(\text{mol\%}) = \frac{a - 5.1159}{0.001547} \tag{2}$$

derived by Ilavsky et al.[11] on the basis of Scott's extended data of analysed YSZ powders with different yttria content with the unit cell dimension a in angstrom at room temperature. Using our value $a = 5.1275(5)$ Å at $T = 20\,^{\circ}C$ a content of 3.7(1) mol% Y_2O_3 is obtained for the cubic phase of the sample taken from

Table 4
Linear thermal expansion coefficients ($\times 10^{-6}\,K^{-1}$).

Phase designation nominal Y_2O_3 content	α_{11}	α_{22}	α_{33}	α_{13}	Temperature interval [°C]	References
ZrO_2 (m) [a,b]	9.0	1.2	11.9	0.0	20–900	Touloukian et al.[5]
ZrO_2 (t)	12.35		14.35	–	1150–1700	Lang[6]
2 mol% (t-YSZ)	8.2–9.0		10.5–13.0	–	25–600–800	Schubert[7]
3 mol% (t-YSZ)	9.3–10.0		10.9–11.6	–	25–600–800	Schubert[7]
9.4, 15, 18, 21, 24 mol% (c-YSZ)[b]	9.0			–	20–1000	Terblanche[8]
3.3 mol% (t′-YSZ)	9.3(2)		10.8(1)	–	60–900	This work
3.7 mol% (c-YSZ)	8.5(2)			–	60–900	This work

[a] Monoclinic axis $2||\vec{a}_2$ (second setting).
[b] Thermal expansion values estimated from published lattice parameter changes.

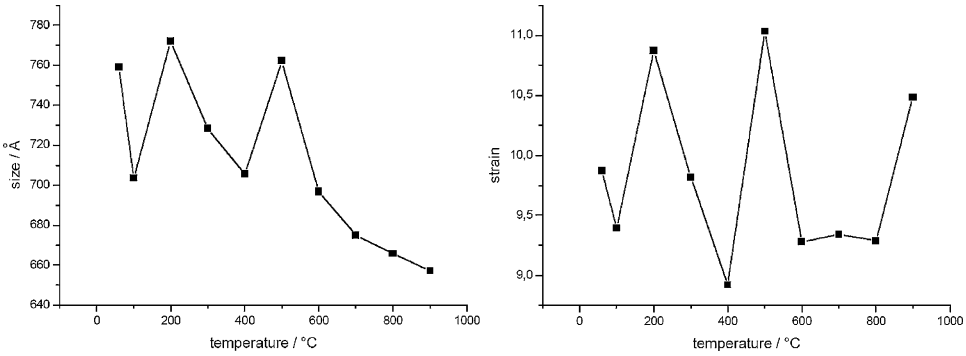

Fig. 5. Grain size and strain plotted as function of temperature. *Note*: Zero-point is suppressed.

the α-Al_2O_3 substrate. Using formula (2) for the cubic modification of the sample taken from the cooled metallic substrate with $a = 5.1276(5)$ Å at $T = 20\,^{\circ}C$ a higher content of 5.9(1) mol% Y_2O_3 is obtained.

Thermal expansion for cubic samples with higher yttria contents was measured by Terblanche.[8] He derived the following lattice parameter equation for cubic YSZ valid from ambient temperatures to 1000 °C:

$$a = 5.1208 + 0.00231y + 4.6468 \times 10^{-5}T + 7.6613 \times 10^{-9}T^2 \quad (3)$$

with y is the mol% Y_2O_3 ($y = 9.4$, 15, 18, 21, 24) and T is the temperature in [°C].

The thermal expansion data determined in this study for the cubic modification from the α-Al_2O_3 substrate, stabilized with a lower content of yttria, shows no significant difference to Terblanche's values.

Structurally the tetragonal t′-YSZ modifications are closely related to the isotropic c-YSZ modifications. The refined lattice parameters at room temperature for the tetragonal phase in this study are in excellent agreement with those published by Ilavsky and Stalick.[9] Furthermore, excellent agreement of lattice parameter a_1 and reasonable agreement of a_3 at 20, 600, and 800 °C can be stated between our data and that of Schubert.[7]

Vegard's law for the tetragonal phase was also derived by Ilavsky et al.,[11] which correlates the yttria content with the ratio of $a_3/\sqrt{2}a_1$

$$YO_{1.5}\ (\text{mol\%}) = \left(1.0225 - \frac{a_3}{\sqrt{2}a_1}\right)/0.0016 \quad (4)$$

with the a_1 and a_3 lattice parameters of the unit cell in angstrom at room temperature. Inserting our values $a_1 = 3.6055(3)$ Å and $a_3 = 5.1596(3)$ Å at $T = 20\,^{\circ}C$ yields a content of 3.3(1) mol% Y_2O_3 for the tetragonal phase of the sample from the α-Al_2O_3 substrate, which is somewhat below the nominal yttria content of 4 mol%. The t′-YSZ modification from the cooled metallic subtrate with $a_1 = 3.6100(1)$ Å and $a_3 = 5.1644(3)$ Å at $T = 20\,^{\circ}C$ leads also to a content of 3.3(1) mol% Y_2O_3. Comparing our results of the thermal expansion coefficients of the tetragonal phase with the values of Schubert[7] it becomes evident that thermal expansion is only marginally influenced by the yttria content, as is the case of the cubic phase (cf. Table 4).

Surprisingly during our high temperature XRD experiments the tendency of an irreversible shift in the phase content from tetragonal (t′) to cubic (c) becomes obvious. This aging process is thermally activated. It is remarkable, that the shift in phase content (t′) → (c) already proceeded at low temperatures as a nearly continuous process over the temperature range from 60 to 900 °C with a rate of d(c)/dT ≈0,15%/h. Phase instabilities in YSZ according to the reaction (t′) → (t) + (c) take place to a significant extend at temperatures above 1200 °C and had been already investigated in earlier publications by Schulz[12] and by Witz et al.[10] Annealing above 900 °C, e.g. at 1150 °C, would have initiated this reaction, which should be avoided in this study.

The linear expansion coefficients of the tetragonal and the cubic phases were found to be close to each other, but significantly different from that of the monoclinic phase which, in addition, shows a pronounced anisotropy (cf. Table 4). As a consequence, shifts in the phase content from tetragonal (t′) to cubic (c) lead to volume changes below 1‰. Therefore the two phases (t′) and (c) are mechanically compatible when subjected to temperature changes and a ceramic sample is only marginally influenced by this phase change. In contrast to the (t′), (t) and (c) phases the monoclinic phase (m) exhibits pronounced anisotropy of the thermal expansion coefficient with a factor of 10 between α_{22} and α_{33} according to Touloukian et al.[5] (cf. Table 4). Consequently, a phase mixture including the monoclinic phase is proune to high volume expansion of several percent, which leads to blistering of TBCs. A martensitic transformation from a tetragonal phase (t) (stabilized with a lower content of yttria) to the monoclinic phase implicates an anisotropic spatialise behaviour and thermal expansion may therefore lead to failure.

4. Conclusion

Precision high temperature X-ray diffraction as a classical method for evaluating thermal expansion coefficients of cubic and tetragonal YSZ phases was applied in this study. The temperature dependent measurements were evaluated via Rietveld's method. The resulting thermal expansion coefficients of the

cubic and tetragonal phases are very similar to each other, and moreover, nearly independent of the yttria content. But they differ significantly from the monoclinic phase. Thus, a solid ceramic component consisting of a mixture of cubic and tetragonal phases is well suited for technical applications at elevated temperatures, as long as the formation of the monoclinic phase can be avoided, because it exhibits a completely different thermal expansion behaviour and causes failure of the components.

During our X-ray experiment, it was recognized that a small relative fraction of phase (t′) was transformed to phase (c) (relative increase of about 3 wt %), as clearly detected in the Rietveld refinements of the X-ray data sets. But the refinements did not give evidence for the simultaneous formation of another tetragonal phase (t) with slightly lower Y_2O_3 content as compared to (t′) according to the decomposition reaction (t′) → (t) + (c), observed at temperatures above 1100 °C, where the thermodynamically stable phase (t) appeared. The analysis of the temperature dependent FWHM values lead to the conclusion that there was a narrow grain-size distribution between 650 and 780 Å and only very little residual strain variation with increasing temperature in our YSZ samples. The latter fact was attributed to (i) the very similar thermal expansion coefficients of the coexisting phases (t′) and (c) and (ii) the absence of phase transformations from any tetragonal phase (t′) or (t) to the monoclinic phase (m).

Our results on thermal expansion of the YSZ phases (t′) and (c) were compared with data of the phases (t), (c), and (m) from the literature and discussed in view of deformation, microstructure and crack formation in TBC layers deposited by EB-PVD: The thermal expansion coefficients of the tetragonal phases (t′) (3.3 mol% Y_2O_3, this work) and (t) (3 mol% Y_2O_3, Schubert[7]) were in excellent agreement with each other likewise the values for the cubic phase (c) obtained in this study (3.7 mol% Y_2O_3) and measured by Terblanche[8] (between 9.4 and 24 mol% Y_2O_3). Furthermore, the thermal expansion coefficients of the tetragonal and cubic phases were very similar to each other although their Y_2O_3 contents were quite different.

An important result of our study is: A phase assemblage of the three phases (t′) and (t) and (c) should not generate critical internal stresses due to their different expansion coefficients to produce damage within an even dense ceramic YSZ layer when subjected to temperature changes up to 1000 °C, provided that no phase transformation to the monoclinic phase (m) occurred. It is the monoclinic phase (m) that would cause damage and lead to failure of the components due to (i) the dramatically different thermal expansion behaviour compared to (t′), (t) and (c), and (ii) the reversible martensitic phase transformation of (m) at around 565 °C associated with a significant volume change.

In the literature a wide range of cubic phase content was reported. In some publications presumably this phase was even overlooked. Due to the problem of overlapping reflection lines neutron scattering experiments are generally superior to X-ray diffraction in order to determine precisely the amount of phase (c). This study showed, that the cheaper and widely available X-ray diffraction method can be successfully applied as well, if a sophisticated analysis evaluation like Rietveld's method is applied, instead of standard X-ray evaluation procedures.

References

1. Scott HG. Phase relationships in the zirconia–yttria system. *J Mater Sci* 1975;**10**:1527–35.
2. Kaysser WA, Peters M, Fritscher K, Schulz U. "Processing, Characterization, and Testing of EB-PVD Thermal Barrier Coatings," pp. no. 9-1-9-11 in Thermal Barrier Coatings. AGARD Rept. No. 823. AGARD;1998.
3. Schneider J. *WYRIET, Version 3*. Pöcking; 1994.
4. Haussühl S. *Kristallphysik*. Weinheim: Physik-Verlag; 1983, 5.
5. Touloukian YS, Kirby RK, Taylor RE, Lee TYR. *"Thermal Expansion - Nonmetallic Solids, in Thermophysical Properties of Matter,'*, vol. 13. New York, Washington: IFI/Plenum; 1977. pp. 451–461.
6. Lang SM. Axial thermal expansion of tetragonal ZrO_2 between 1150 and 1700 °C. *J Am Ceram Soc* 1964;**47**(12):641–4.
7. Schubert H. Anisotropic thermal expansion coefficients of Y_2O_3-stabilized tetragonal zirconia. *J Am Ceram Soc* 1986;**69**(3):270–1.
8. Terblanche SP. Thermal-expansion coefficients of yttria-stabilized zirconias. *J Appl Crystallogr* 1989;**22**:283–4.
9. Ilavsky J, Stalick JK. Phase composition and its changes during annealing of plasma-sprayed YSZ. *Surf Coat Technol* 2000;**127**(2-3):120–9.
10. Witz G, Shklover V, Streuer W, Bachegowda S, Bossmann HP. Phase evolution in yttria-stabilized zirconia thermal barrier coatings studied by rietveld refinement of X-ray powder diffraction patterns. *J Am Ceram Soc* 2007;**90**(9):2935–40.
11. Ilavsky J, Stalick JK, Wallace J. Thermal spray yttria-stabilized zirconia phase changes during annealing. *J Therm Spray Technol* 2001;**10**(3):497–501.
12. Schulz U. Phase transformation in EB-PVD yttria partially stabilized zirconia thermal barrier coatings during annealing. *J Am Ceram Soc* 2000;**83**(4):904–10.